Full Length Research Paper

Homology modeling of γ-aminobutyrate-aminotransferase, a pyridoxal phosphate-dependent enzyme of *Homo sapiens*: Molecular modeling approach to rational drug design against epilepsy

Hina Naz Khan[1], Hamid Rashid[1]* and Saima Kulsoom[2]

[1]Department of Bioinformatics, Mohammad Ali Jinnah University, Islamabad, Pakistan.
[2]Department of Chemistry, Quaid-e-Azam University, Pakistan.

γ-Aminobutyrate aminotransferase (GABA-AT) is a pyridoxal phosphate dependent homodimeric enzyme of 50-kD subunits. It is a potential drug target against epilepsy. The three-dimensional structure of GABA-AT is not experimentally known, and we thus resorted to homology modelling to build a model based on x-ray crystal structure of pig liver GABA-AT to 3.0 Å resolution. Knowledge of the three-dimensional structure of GABA-AT would greatly advance the development of novel lead compounds targeting this molecule. The protein's conservity was verified by performing multiple alignments using ClustalW and MUSCLE programs. The model was further checked for its correctness by predicting the 2D and 3D structures, which validates the structure.

Key words: γ-Aminobutyrate aminotransferase (GABA-AT), epilepsy, crystal structure, homology modeling, BLAST, template.

INTRODUCTION

γ-Aminobutyrate aminotransferase, (GABA-AT) (4-amino-butyrate aminotransferase, GABA transferase, GABA aminotransferase, 4-aminobutyrate transaminase and gamma-amino-N-butyrate transaminase) is a pyridoxal phosphate dependent homodimeric enzyme distributed widely in nature (Cooper, 1985). The enzyme GABA-AT has been purified and characterized in several labora-tories (Bloch-Tardy et al., 1974). It is a homodimer of 50-kD subunits, with each subunit containing an active-site PLP covalently bound to Lys-329 via a Schiff base. GABA-AT belongs to a large family of homologous aminotransferases (Mehta et al., 1993) which operate by the same basic mechanism consisting of two coupled half-reactions in which the PLP-cofactor oscillates between its pyridoxal and pyridoxamine forms. Together with the structurally well characterized enzymes ornithine aminotransferase (OAT) and dialkylglycine decarboxylase

(DGD), GABA-AT belongs to the subfamily II of the family of PLP-dependent enzymes (Mehta and Chriten, 2000). The mechanism for GABA-AT is well known (Cooper, 1985). In GABA-AT, the specific reaction converts GABA to succinic semialdehyde (Cooper, 1985). It is a target for neuroactive drugs because its inhibition alters the balance between its substrate GABA and the product L-glutamate, which are respectively the major inhibitory and excitatory neurotransmitters in the brain. Selective inactivation by vinyl-GABA, a mechanism-based inhibitor of the enzyme (Lippert et al., 1977), is already success-fully applied in the treatment of epilepsy (Davies, 1995). In fact, about one-quarter of epileptic patients worldwide (about 12 million people) do not respond to any marketed anticonvulsant drug. Therefore, the need for new anticonvulsant drugs is great (Rogawski and Potter, 1990). A reduction in the concentrations of GABA has been implicated not only in the symptoms associated with epilepsy (Bakay and Harris, 1981) but also with several other neurological diseases such as Huntington's chorea (Butterworth et al., 1993), Parkinson's disease (Nishino et al., 1988), Alzheimer's disease (Aoyagi et al., 1990), and

---

*Corresponding author. E-mail: drhamid@jinnah.edu.pk. Tel: 111-87-87-87.

tardive dyskinesia (Gunne et al., 1984). Administration of GABA peripherally is not effective, because GABA, under normal conditions, cannot cross the blood-brain barrier; however, several other approaches have been taken to increase the brain concentrations of GABA.

In 1999, the x-ray crystal structure of pig liver GABA-AT was reported at 3.0-Å resolution (Storici et al., 2004), which elucidated the active-site geometry and allowed conclusions to be drawn with respect to its specificity. The crystal structure of pig liver GABA-AT, is 96% identical to the human brain enzyme (De Biase et al., 1995). The availability of the GABA-AT structure will assist the rational design of new neuroactive compounds of value in the treatment of the several neurological and psychiatric disorders accompanied by altered GABA levels.

Epilepsy is a neurological condition, which affects the nervous system. It is also known as a seizure disorder (Bell and Sander, 2001). In earlier drug designing, drugs were always used as trial-and-error process. The conventional way of synthesizing drugs has always been a tedious process, consuming several years, huge man power and extremely expensive in order to come up with a single effective novel drug. Estimates of time and cost of currently bringing a new drug to market vary, but 7 to 12 years and $ 1.2 billion are often cited (Shankar et al., 2006). However, now it can be done efficiently *in-silico*, thereby saving huge funds and man power. The pipeline of drug discovery from idea to market consists of seven basic steps: disease selection, target selection, lead compound identification, lead optimization, preclinical trials, clinical trial testing and pharmacogenomic optimization. Knowing the target, that is, the 3D structure of the protein is very important. The 3D structure of protein targets is most often derived from x-ray crystallography or nuclear magnetic resonance (NMR) techniques or even homology modeling. Homology modeling is to build a three dimensional (3D) model for a protein of unknown structure (the target) based on one or more related proteins of known structure (the templates) (Blundell et al., 1987; Greer, 1990; Johnson et al., 1994; Bajorath et al., 1994; Sali, 1995; Sanchez and Sali, 1997). Homology modeling was performed in our study as the x-ray crystallographic structure is not available for GABA-AT of human source. It is an essential requirement for identifying the structural characteristics of this protein as target to find a suitable antiepileptic drug, which is the main objective of our study.

MATERIALS AND METHODS

The sequence of GABA-AT protein (500 amino acids) of human was downloaded for structural modeling from UniProtKB/Swiss-Prot (EC 2.6.1.19). The physical and chemical properties of the sequence were calculated by the program ProtParam. The computed parameters for a given protein includes the molecular weight, theoretical pI, amino acid composition, atomic composition, extinction coefficient, estimated half life, instability index, aliphatic

index and grand average of hydropathicity (GRAVY). Multiple alignments of the related sequences were performed using the online available ClustalW program (http://www.ebi.ac.uk/Tools/clustalw2/index.html) (Thompson et al., 1994) accessible through the European Bioinformatics Institute and MUSCLE, a computer program for creating multiple alignments of protein sequences. Elements of the algorithm include fast distance estimation using kmer counting, progressive alignment using a new profile function we call the log-expectation score, and refinement using tree-dependent restricted partitioning (Edgar, 2004)..

Different servers, that is, TMHMM (Krogh et al., 2001), SOSUI (Hirokawa et al., 1998) and TMpred are programs that make a prediction of membrane-spanning regions and their orientation. The algorithm was based on the statistical analysis of TMbase, a database of naturally occurring transmembrane proteins. The prediction was made using a combination of several weight-matrices for scoring (Hofman and Stoffel, 1993) which were accessed to validate the TM region of GATA-AT protein. TMHMM, a new membrane protein topology prediction method, is based on a hidden Markov model. The prediction of protein secondary structure is an important step for the prediction of protein's tertiary structure. Secondary structure of GABA-AT was taken from the JPRED, a server powered by the Jnet algorithm. The algorithm provides a three-state (a-helix, b-strand and coil) prediction of secondary structure at an accuracy of 81.5% (Cole et al., 2008). PSIPRED, a server that is able to complete predictions in most cases in less than 2 min and processes about 100 predictions, requires a day and produces two dimensional graphical results (McGuffin et al., 2000). SABLE, a server for improved prediction of secondary structures uses evolutionary profiles and predicts relative solvent accessibility of an amino acid residue as a fingerprint of the overall packing (Adamczak et al., 2005) and PredictProtein , provides PROSITE sequence motifs, low complexity regions (SEG), nuclear localization signals, regions lacking regular structure (NORS) and predictions of secondary structure, solvent accessibility, globular regions, transmembrane helices, coiled-coil regions, structural switch regions, disulfide-bonds, sub-cellular localization, and functional annotations (Puntervoll et al., 2003; Rost et al., 2004; Bairoch et al., 1997; Ceroni et al., 2004). Comparison of the results of respective programs was performed.

No x-ray crystallographic or NMR structure of this protein of human source has been determined, therefore homology modeling was performed. The process of building a comparative model is conceptually straight forward. The methodology itself can be described in four steps; identifying a suitable template, making an optimal target-template alignment, building the model and validating the model. The comparative model of GABA-AT was built using a web-based homology-modeling server,

SWISS-MODEL (Jain, 2004; Stoermer, 2006) and MODWEB, a comparative modeling server is integrated as a module in MODBASE (Pieper et al., 2009). Models are built using comparative modeling by satisfaction of spatial restraints as implemented in Modeller (Sali and Blundell, 1993). Homology Modeling is performed in the following steps: Firstly, it searches for suitable template for the submitted protein by using BLAST program. In the second step, it selects the suitable templates with sequence identity of above 25%. The accuracy of a model depends upon the sequence similarity it shares with the template. Models with >50% sequence identity to templates are normally of high quality, with ~1 Å root mean square (RMS) error for main chain atoms (equal to medium-resolution NMR or low resolution x-ray structures). Models that have 30 to 50% sequence identity are normally of medium accuracy with an RMS of ~1.5 Å (Kasteleijn-Nolst et al., 2007; Enyedy et al., 2001). Thirdly, once the 3D model is created, the important step and last step is evaluating the 3D model of the protein. Structure validation was performed using ANOLEA (http://www.fundp.ac.be/pub/ANOLEA.html), VERIFY-3D (Holm and Sander, 1992) and GROMOS 96 of SWISS-PDB server. The model

Table 1. Multiple alignment score of GABA-AT protein.

Sequence	Name and length of amino acids	Alignment	Score (%)
1	Homo Sapiens (500)	Sequences (1:2), Sequences (1:3), Sequences (1:4), Sequences (1:5), Sequences (1:6), Sequences (1:7), Sequences (1:8), Sequences (1:9)	94, 91, 91, 51, 44, 41 40, 40
2	Bos Taurus (500)	Sequences (2:3), Sequences (2:4), Sequences (2:5), Sequences (2:6), Sequences (2:7), Sequences (2:8), Sequences (2:9)	91, 91, 51, 45, 40, 40, 40
3	*Mus musculus* (500)	Sequences (3:4), Sequences (3:5), Sequences (3:6) Sequences (3:7), Sequences (3:8), Sequences (3:9)	97, 50, 44, 41, 40, 40
4	*Rattus norvegicus* (500)	Sequences (4:5), Sequences (4:6), Sequences (4:7) Sequences (4:8) Sequences (4:9)	50, 44, 40, 40, 40
5	*Drosophila* (486)	Sequences (5:6), Sequences (5:7), Sequences (5:8) Sequences (5:9)	48, 42, 46, 44
6	*Caenorhabditis* (483)	Sequences (6:7), Sequences (6:8) Sequences (6:9)	43, 43, 41
7	*Schizosaccharomyces* (474)	Sequences (7:8), Sequences (7:9)	47, 46
8	*Saccharomyces* (471)	Sequences (8:9)	73
9	*Ashbya gossypii* (483)		

obtained by MODWEB was verified by different programs provided on the platform of Structural Analysis and Verification Server (SAVES) (http://nihserver.mbi.ucla.edu/SAVES). We selected PROCHECK (Laskowski et al., 1993) and VERIFY_3D among the available programs on SAVES to evaluate the quality of our model. The solvation profile of the protein structure was obtained using SolvX server. It is useful for assessing the quality of a homology model. The model was visualized using VMD and Rasmol visualization softwares.

RESULTS AND DISCUSSION

General information of protein

The sequence of GABA-AT was analyzed by the computer program Protparam in order to find the physical and chemical properties. The number of amino acids was 500, molecular weight was 56438.9 and theoretical pI was 8.17. The amino acid composition showed that, the number of leucine (L) was the highest, that is, 49 (9.8%), number of negatively charged residues (aspartic acid and glutamic acid) was 57, number of positively charged residues (Arginine, Lysine) was 60, instability index was 42.12 which classifies the protein as unstable, aliphatic index was 83.52 and the grand average of hydropathicity was -0.265.

Multiple sequence alignment of amino acid sequences of GABA-AT protein of different organisms (*Homo sapiens*, *Bos taurus*, *Mus musculus*, *Rattus norvegicus*, *Drosophila melanogaster*, *Caenorhabditis elegans*, *Schizosaccharomyces pombe*, *Saccharomyces cerevisiae*

and *Ashbya gossypii*) showed that they are very close to each other ranging from 40 to 97 % as shown in Table 1. Figure 1 shows the result of the multiple sequence alignment of the mentioned organisms using CLUSTALW program. Multiple alignment of GABA-AT protein shows that *M. musculus* and *R. norvegicus* had 97% identity as shown in Figure 1. From the cladogram, GABA-AT protein of *R. norvegicus* was found to be far from that of *A. gossypii* (Figure 2).

Transmembrane helices

Different servers were accessed for accurate prediction analysis of transmembrane region such as TMHMM, SOSUI and TMpred. The possible transmembrane helices of the sequence were from positions 202 to 225 with score 225; 150 to 179 with score 132 and 210 to 226 with score 555. Only scores above 500 were considered significant, that is, only one strong transmembrane was present with score 555.

Table 2 summarizes the result of TMpred showing the significant possible transmembrane helices and Figure 3 shows the transmembrane helices. The principal idea underlying most secondary structure prediction methods is the fact that segments of con-secutive residues have preferences for certain secondary structure states. Performance accuracy seemed to have been limited to about 60%. The limited accuracy was argued to result from the fact that all the methods used only information that were local in sequence.
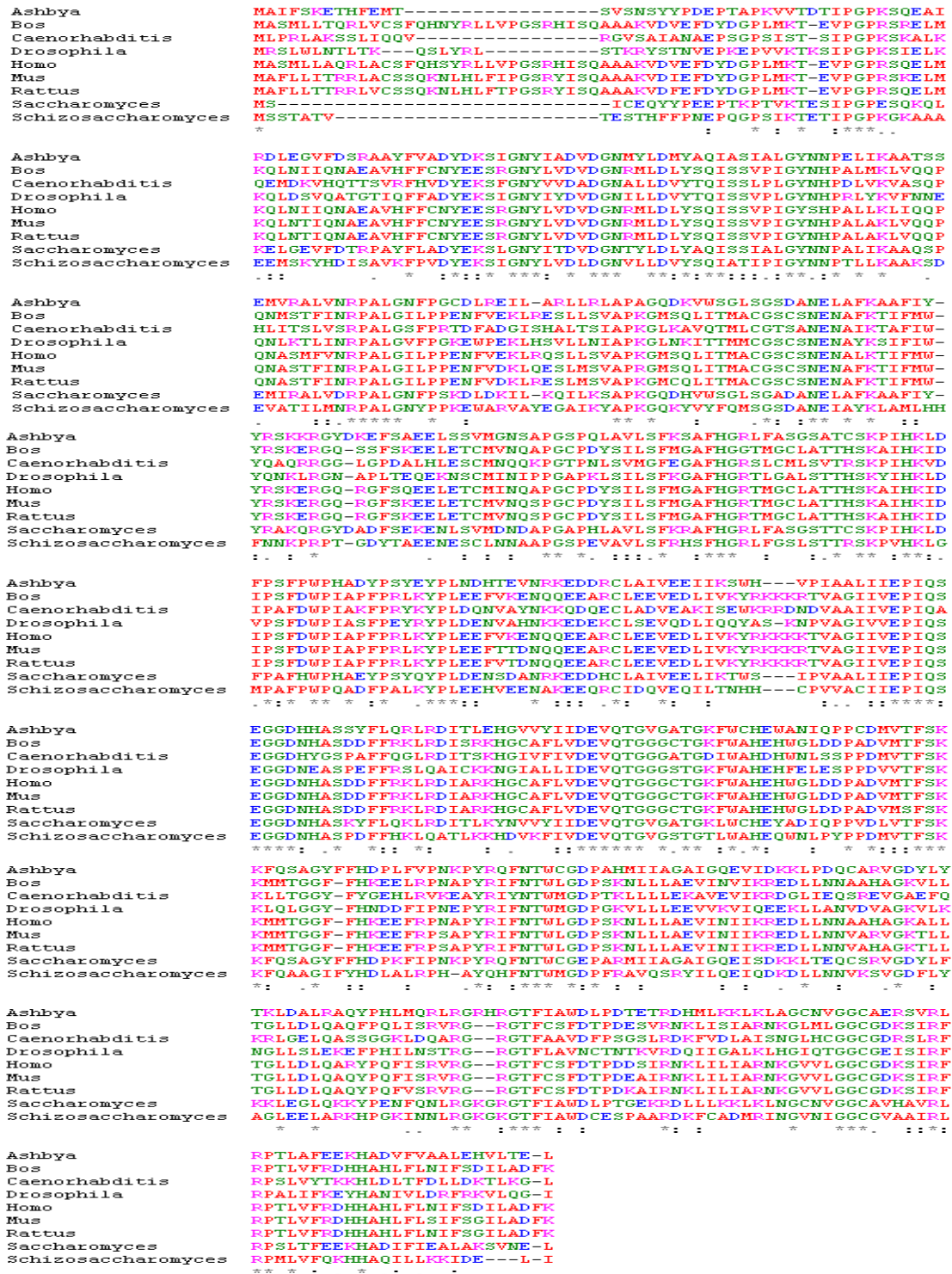
```
Ashbya             MAIFSKETHFEMT----------------SVSNSYYPDEPTAPKVVTDTIPGPKSQEAI
Bos                MASMLLTQRLVCSFQHNYRLLVPGSRHISQAAAKVDVEFDYDGPLMKT-EVPGPRSRELM
Caenorhabditis     MLPRLAKSSLIQQV---------------RGVSAIANAEPSGPSIST-SIPGPKSKALK
Drosophila         MRSLWLNTLTK---QSLYRL----------STKRYSTNVEPKEPVVKTKSIPGPKSIELK
Homo               MASMLLAQRLACSFQHSYRLLVPGSRHISQAAAKVDVEFDYDGPLMKT-EVPGPRSQELM
Mus                MAFLLITRRLACSSQKNLHLFIPGSRYISQAAAKVDIEFDYDGPLMKT-EVPGPRSKELM
Rattus             MAFLLTTRRLVCSSQKNLHLFTPGSRYISQAAAKVFEFDYDGPLMKT-EVPGPRSQELM
Saccharomyces      MS-------------------------ICEQYYPEEPTKPTVKTESIPGPESQKQL
Schizosaccharomyces MSSTATV---------------------TESTHFFPNEPQGPSIKTETIPGPKGKAAA
                   *                            :   *  :  *   :***..

Ashbya             RDLEGVFDSRAAYFVADYDKSIGNYIADVDGNMYLDMYAQIASIALGYNNPELIKAATSS
Bos                KQLNIIQNAEAVHFFCNYEESRGNYLVDVDGNRMLDLYSQISSVPIGYNHPALMKLVQQP
Caenorhabditis     QEMDKVHQTTSVRFHVDYEKSFGNYVVDADGNALLDVYTQISSLPLGYNHPDLVKVASQP
Drosophila         KQLDSVQATGTIQFFADYEKSIGNYIYDVDGNILLDVYTQISSVPLGYNHPRLYKVFNNE
Homo               KQLNIIQNAEAVHFFCNYEESRGNYLVDVDGNRMLDLYSQISSVPIGYSHPALLKLIQQP
Mus                KQLNTIQNAEAVHFFCNYEESRGNYLVDVDGNRMLDLYSQISSVPIGYNHPALAKLVQQP
Rattus             KQLNTIQNAEAVHFFCNYEESRGNYLVDVDGNRMLDLYSQISSVPIGYNHPALAKLVQQP
Saccharomyces      KELGEVFDTRPAYFLADYEKSLGNYITDVDGNTYLDLYAQISSIALGYNNPALIKAAQSP
Schizosaccharomyces EEMSKYHDISAVKFPVDYEKSIGNYLVDLDGNVLLDVYSQIATIPIGYNHPTLLKAAKSD
                   .:  *      :*  *   :*::* ***: *  *** **:*:**:::.:**.:*  *  *

Ashbya             EMVRALVNRPALGNFPGCDLREIL-ARLLRLAPAGQDKVWSGLSGSDANELAFKAAFIY-
Bos                QNMSTFINRPALGILPPENFVEKLRESLLSVAPKGMSQLITMACGSCSNENAFKTIFMW-
Caenorhabditis     HLITSLVSRPALGSFPRTDFADGISHALTSIAPKGLKAVQTMLCGTSANENAIKTAFIW-
Drosophila         QNLKTLINRPALGVFPGKEWPEKLHSVLLNIAPKGLNKITTMMCGSCSNEWAYKSIFIW-
Homo               QNASMFVNRPALGILPPENFVEKLRQSLLSVAPKGMSQLITMACGSCSNENALKTIFMW-
Mus                QNASTFINRPALGILPPENFVDKLQESLMSVAPRGMSQLITMACGSCSNENAFKTIFMW-
Rattus             QNASTFINRPALGILPPENFVDKLRESLMSVAPKGMCQLITMACGSCSNENAFKTIFMW-
Saccharomyces      EMIRALVDRPALGNFPSKDLDKIL-KQILKSAPKGQDHVWSGLSGADANELAFKAAFIY-
Schizosaccharomyces EVATILMNRPALGNYPPKEWARVAYEGAIKYAPKGQKYVYFQMSGSDANEIAYKLAMLHH
                   -      ::.*****  *   :      ** *. :::.*  **** * * *  ::

Ashbya             YRSKKRGYDKEFSAEELSSVMGNSAPGSPQLAVLSFKSFASGSATCSKPIHKLD
Bos                YRSKERGQ-SSFSKEELETCMVNQAPGCPDYSILSFMGAFHGGTMGCLATTHSKAIHKID
Caenorhabditis     YQAQRRGG-LGPDALHLESCMNQQKPGTPNLSVMGFEGAFHGRSLCMLSVTRSKPIHKVD
Drosophila         YQNKLRGN-APLTEQEKNSCMINIPPGAPKLSILSFKGAFHGRTLGALSTTHSKYIHKLD
Homo               YRSKERGQ-RGFSQEELETCMINQAPGCPDYSILSFMGAFHGRTMGCLATTHSKAIHKID
Mus                YRSKERGQ-RGFSKEELETCMVNQSPGCPDYSILSFMGAFHGRTMGCLATTHSKAIHKID
Rattus             YRSKERGQ-RGFSKEELETCMVNQSPGCPDYSILSFMGAFHGRTMGCLATTHSKAIHKID
Saccharomyces      YRAKQRGYDADFSEKENLSVMDNDAPGAPHLAVLSFKRAFHGRLFASGSTTCSKPIHKLD
Schizosaccharomyces FNNKPRPT-GDYTAEENESCLNNAAPGSPEVAVLSFRHSFHGRLFGSLSTTRSKPVHKLG
                   :. : *   .      :    : :    ** *. :::.*  :****  :    :.* ** :***:.

Ashbya             FPSFPWPHADYPSYEYPLNDHTEVNRKEDDRCLAIVEEIIKSWH---VPIAALIIEPIQS
Bos                IPSFDWPIAPFPRLKYPLEEFVKENQQEEARCLEEVEDLIVKYRKKKRTVAGIIVEPIQS
Caenorhabditis     IPAFDWPIAKFPRYKYPLDQNVAYNKKQDQECLADVEAKISEWKRRDNDVAAIIVEPIQA
Drosophila         VPSFDWPIASFPEYRYPLDENVAHNKKEDEKCLSEVQDLIQQYAS-KNPVAGIVVEPIQS
Homo               IPSFDWPIAPFPRLKYPLEEFVKENQQEEARCLEEVEDLIVKYRKKKRTVAGIIVEPIQS
Mus                IPSFDWPIAPFPRLKYPLEEFTTDNQQEEARCLEEVEDLIVKYRKKKRTVAGIIVEPIQS
Rattus             IPSFDWPIAPFPRLKYPLEEFVTDNQQEEARCLEEVEDLIVKYRKKKRTVAGIIVEPIQS
Saccharomyces      FPAFHWPHAEYPSYQYPLDENSDANRKEDDHCLAIVEELIKTWS---IPVAALIIEPIQS
Schizosaccharomyces MPAFWPWPQADFPALKYPLEEHVEENAKEEQRCIDQVEQILTNHH---CPVVACIIEPIQS
                   .*:.* ** * :*  .***::    * :::.:  *:  *:  :       :.. ::****:

Ashbya             EGGDHHASSYFLQRLRDITLEHGVVYIIDEVQTGVGATGKFWCHEWANIQPPCDMVTFSK
Bos                EGGDNHASDDFFRKLRDISRKHGCAFLVDEVQTGGGCTGKFWAHEHWGLDDPADVMTFSK
Caenorhabditis     EGGDHYGSPAFFQGLRDITSKHGIVFIVDEVQTGGGDATGDIWAHDHWNLSSPPDMVTFSK
Drosophila         EGGDNEASPEFFRSLQAICKKHGIALLIDEVQTGGGSTGKFWAHEHFELESPPDVVTFSK
Homo               EGGDNHASDDFFRKLRDIARKHGCAFLVDEVQTGGGCTGKFWAHEHWGLDDPADVMTFSK
Mus                EGGDNHASDDFFRKLRDIARKHGCAFLVDEVQTGGGCTGKFWAHEHWGLDDPADVMTFSK
Rattus             EGGDNHASDDFFRKLRDIARKHGCAFLVDEVQTGGGCTGKFWAHEHWGLDDPADVMSFSK
Saccharomyces      EGGDNHASKYFLQKLRDITLKYNVVYIIDEVQTGVGATGKLWCHEVYADIQPPVDLVTFSK
Schizosaccharomyces EGGDNHASPDFFHKLQATLKKHDVKFIVDEVQTGVGSTGTLWAHEQWNLPYPPDMVTFSK
                   ****:   .*  *:: *:     : .  :::******* *.** :*.*:    :   * *:::***

Ashbya             KFQSAGYFFHDPLFVPNKPYQFNTWCGDPAHMIIAGAIGQEVIDKKLPDQCARVGDYLY
Bos                KMMTGGF-FHKEELRPNAPYRIFNTWLGDPSKNLLLAEVINVIKREDLLNNAAHAGKVLL
Caenorhabditis     KLLTGGY-FYGEHLRVKEAYRIYNTWMGDPTKLLLLEEKAVHRIRDGLIEQSREVGAEFQ
Drosophila         KLQLGGY-FHNDDFIPNEPYRIFNTWMGDPGKVLLLEEVVKVIQEEKLLANVDVAGKVLK
Homo               KMMTGGF-FHKEEFRPNAPYRIFNTWLGDPSKNLLLAEVINIIKREDLLNNAAHAGKALL
Mus                KMMTGGF-FHKEEFRPSAPYRIFNTWLGDPSKNLLLAEVINIIKREDLLNNVARVGKTLL
Rattus             KMMTGGF-FHKEEFRPSAPYRIFNTWLGDPSKNLLLAEVINIIKREDLLNNVAHAGKTLL
Saccharomyces      KFQSAGYFFHDPKFIPNKPYRQFNTWCGEPARMIIAGAIGQEISDKKLTEQCSRVGDYLF
Schizosaccharomyces KFQAAGIFYHDLALRPH-AYQHFNTWMGDPFRAVQSRYILQEIQDKDLLNNVKSVGDFLY
                   *:  . * ::   :    .*: :***  *  *: :    .*   :. * :  .  *

Ashbya             TKLDALRAQYPHLMQRLRGRHRGTFFIAWDLPDTETRDHMLKKLKLAGCNVGGCAERSVRL
Bos                TGLLDLQAQFPQLISRVRG--RGTFCSFDTPDESVRNKLISIARNKGLMLGGCGDKSIRF
Caenorhabditis     KRLGELQASSGGKLDQARG--RGTFAAVDFPSGSLRDKFVDLAISNGLHCGGCGDRSLRF
Drosophila         NGLLSLEKEFPHILNSTRG--RGTFLAVNCTNTKVRDQIIGALKLHGIQTGGCGEISIRF
Homo               TGLLDLQAQYPQFISRVRG--RGTFCSFDTPDDSIRNKLILIARNKGVVLGGCGDKSIRF
Mus                TGLLDLQAQYPQFISRVRG--RGTFCSFDTPDEAIRNKLILIARNKGVVLGGCGDKSIRF
Rattus             TGLLDLQAQYPQFVSRVRG--RGTFCSFDTPDKAIRNKLILIARNKGVVLGGCGDKSIRF
Saccharomyces      KKLEGLQKKYPENFQNLRGKGRGTFIAWDLPTGEKRDLLLKKLKLNGCNVGGCAVHAVRL
Schizosaccharomyces AGLEELARKHPGKINNLRGKGKGTFIAWDCESPAARDKFCADMRINGVNIGGCGVAAIRL
                   .      .. **  :*** ::*.  :    *:.     * : .*  *

Ashbya             RPTLAFEEKHADVFVAALEHVLTE-L
Bos                RPTLVFRDHHAHLFLNIFSDILADFK
Caenorhabditis     RPSLVYTKKHLDLTFDLLDKTLKG-L
Drosophila         RPALIFKEYHANIVLDRFRKVLQG-I
Homo               RPTLVFRDHHAHLFLNIFSDILADFK
Mus                RPTLVFRDHHAHLFLSIFSGILADFK
Rattus             RPTLVFRDHHAHLFLNIFSGILADFK
Saccharomyces      RPSLTFEEKHADIFIEALAKSVNE-L
Schizosaccharomyces RPMLVFQKHHAQILLKKIDE---L-I
                   ** * *: . : * :*.: .  :
```

**Figure 1.** Multiple alignment score of amino acid sequences of GABA-AT protein of the different organisms

Secondary structure prediction

There are several programs available to predict the secondary structure. We selected the following servers in order to predict the secondary structure: PSIPRED, JPRED, PredictProtein and SABLE. Table 3 shows the result of the different servers; it shows the location of helices, sheets and coils. There was a minute difference in the positions of the helices, sheet and coils but it was negligible. The consensus regions of alpha helices, beta
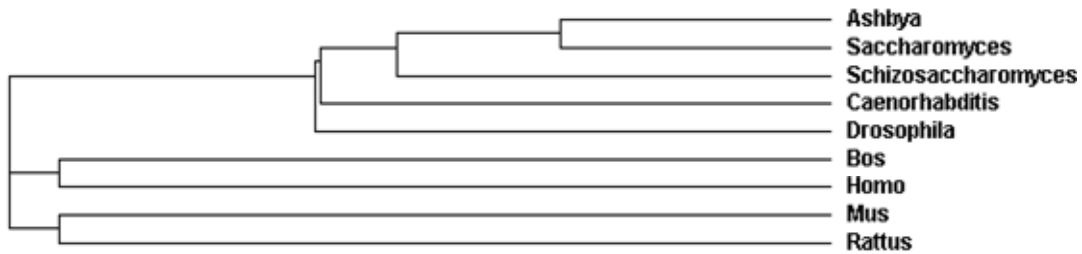
Figure 2. Cladogram showing phylogenetic relationship of GABA-AT protein of different organisms having GABA-AT protein.
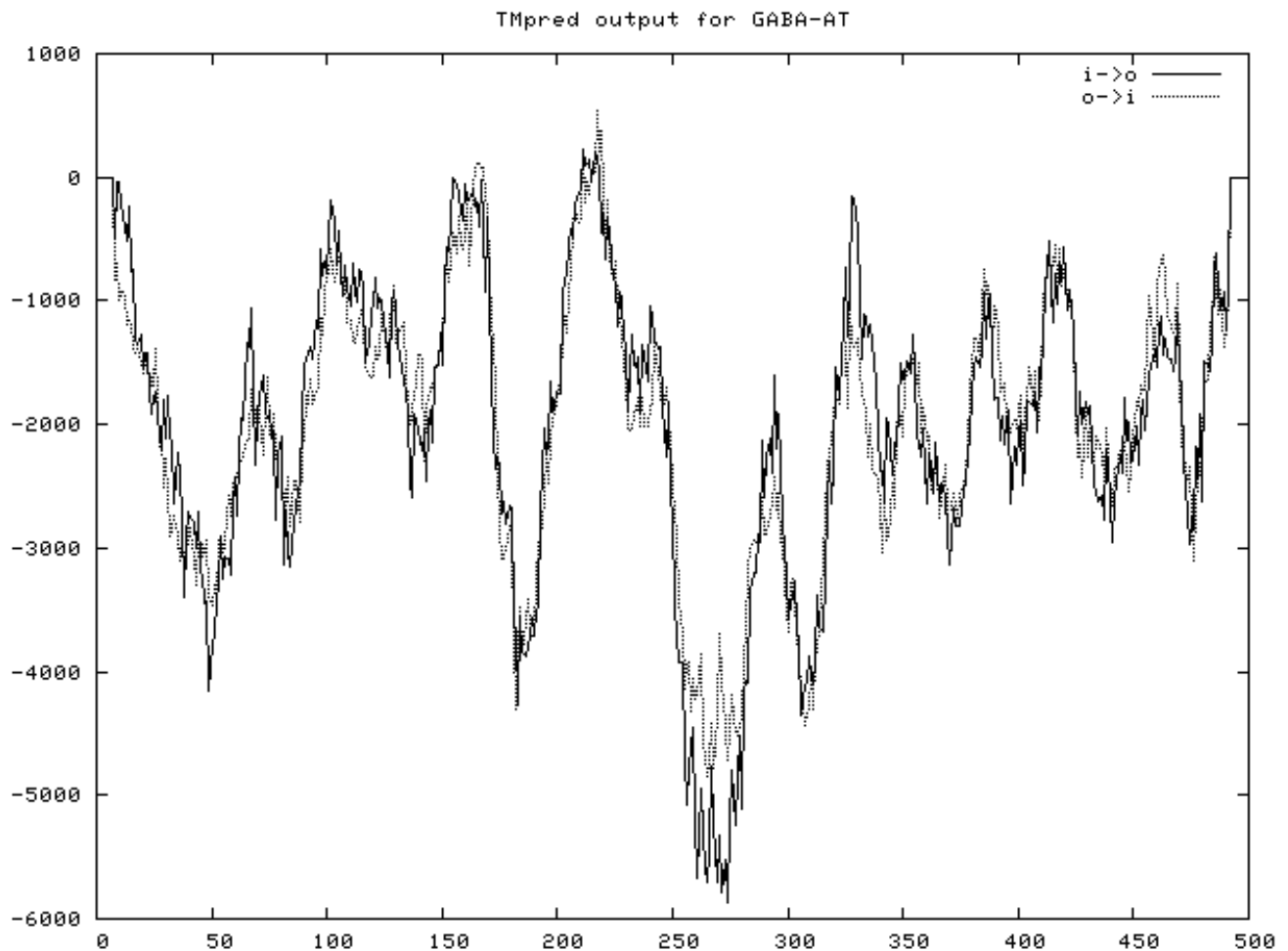
Figure 3. Graphical view of transmembrane helices.

Table 2. Significant possible transmembrance helices of GABA-AT; only scores above 500 are considered significant.

S/N	Strong transmembrane helix		
	From	**To**	**score**
1	202	225	225
2	150	179	132
3	210	226	555

strands and coils for the three servers were chosen which are as follows: residues 3 to 12, 28 to 34, 100 to 104, 110 to 124, 136 to 150, 166 to 181, 220 to 229, 306 to 320, 326 to 342, 363 to 370, 383 to 400, 401 to 425, 444 to 460 and 478 to 499 were involved in the alpha-helices formation, residues from 75 to 81, 83 to 88, 92 to 97, 156 to 163, 209 to 216, 289 to 295, 319 to 336, 349 to 359, 433 to 444, 459 to 466 and 467 to 476 were involved in

Table 3. Secondary structure prediction.

Helix			Sheet			Coil		
JPRED	PSIPRED	SABLE	JPRED	PSIPRED	SABLE	JPRED	PSIPRED	SABLE
3-8	4-15	3-10	75-79	76-82	74-79	1-2	1-3	1-2
28-34	28-33	28-34	83-87	85-88	84-87	9-52	34-53	35-54
100-104	54-67	55-62	92-97	93-97	92-97	65-74	68-75	63-73
110-122	100-104	110-122	156-160	159-163	156-160	105-109	105-110	104-109
136-149	110-126	136-150	209-214	211-216	209-213	123-135	127-137	123-135
166-181	138-152	165-180	287-293	289-295	287-293	150-155	153-158	151-155
222-226	166-184	219-227	319-323	324-328	332-336	182-191	185-192	181-208
306-315	220-230	264-280	349-359	354-357	352-355	197-265	231-263	228-263
326-330	264-283	306-328	433-440	431-440	439-444	283-286	284-288	281-286
363-366	308-320	336-342	459-461	465-467	463-466	294-305	296-307	294-305
383-397	340-345	364-370	467-471	473-476	471-475	331-348	329-339	327-336
401-422	369-372	386-401				354-362	346-353	356-363
444-455	388-403	405-425				367-378	373-387	371-385
478-494	406-427	450-459				398-400	428-430	445-448
	449-462	482-500				423-432	434-439	460-462
	483-500					441-458	477-482	467-470
						462-466		476-481
						472-477		

Beta strands formation, whereas residues from 1 to 3, 34 to 54, 65 to 75, 105 to 110, 123 to 137, 150 to 110, 123 to 137, 150 to 158, 182 to 208, 231 to 263, 283 to 286, 294 to 307, 331 to 348, 354 to 362, 367 to 387, 423 to 430, 441 to 458, 462 to 470 and 472 to 481 were involved in coils formation.

3D structure prediction via homology modeling

We employed a homology search in PDB database using BLAST and PSIBLAST to identify potential templates. The significant templates obtained were of *Sus scrofa* (pig) with 95.87% identity, *B. taurus* (bovine) with 94% identity, *R. norvegicus* (rat) with 91% identity and *M. musculus* (mouse) with 91% identity. However, we selected GABT_PIG (SWISS ID: P80147, PDB ID: 1OHV) as a template for GABA-AT modeling because its crystal structure has been reported. After identification of the best template for modelling, an optimal alignment was made. This seems to be the most crucial step in homology modeling. Here "optimal" means that corresponding sequence positions in target and template were identified, so that the predicted structure of the target, based on the template, is as similar as possible to an experimental structure of the same target. Pair-wise comparison between the target GABA-AT amino acid sequence with the template amino acid sequence of GABT_PIG indicate approximately 95% identity as shown in Figure 4. The three-dimensional structure of a protein is a key to understanding its function. Once the template is selected on an alignment performed, target on template was mapped which transfers the coordinates from the template to the target of structurally conserved regions. Figure 5 shows the 3D structure of GABA-AT using SWISSMODEL. Homolgy Modeling performed by MODWEB showed the following result: the template structure used by MODWEB had a PDB id 1ohv. The sequence identity which shows the percentage of identical residues between the template and target alignment was shown to be 96% for our target sequence. Here the sequence identity result was 96% which is a positive sign towards accurate model having the best possible template. The model reliability score known as Model Score for our target sequence was 1.00. If a model score is higher than a pre-specified cutoff (0.7), then the predicted model is considered to be a good model. The template modeled residue range was 39 to 499.

The MODPIPE protein quality score (MPQS) which is a composite score based upon the sequence identity of target to template, coverage and three scores (e-value, z-Dope and GA341) for our protein was 2.14803. The MPQS greater than 1.1 is considered to be reliable (Pieper et al., 2004). The sequence model coverage which shows the modeled area of the target sequence was represented by different colors. The significance of best model is shown by colors. The model coverage sketch had 4 lines. The top line represents the sequence identity of template with the target and if it is greater than 30%, it is shown by green color and if less than 30%, it is represented by red color .The second line which represents the template to target E-value is shown by green if E-value < = 0.0001 and is shown by red if E-value >0.0001. The model score is represented by the

```
P80147    MASVLLTRRLACSFRHNHRLLVPGWRHISQAAAKVDVEFDYDGPLMKTEVPGPRSRELMK    60    GABT_PIG
P80404    MASMLLAQRLACSFQHSYRLLVPGSRHISQAAAKVDVEFDYDGPLMKTEVPGPRSQELMK    60    GABT_HUMAN
          ***:**:;*****:.*.:****** ********************************:****

P80147    QLNIIQNAEAVHFFCNYEESRGNYLVDVDGNRMLDLYSQISSIPIGYSHPALVKLVQQPQ    120   GABT_PIG
P80404    QLNIIQNAEAVHFFCNYEESRGNYLVDVDGNRMLDLYSQISSVPIGYSHPALLKLIQQPQ    120   GABT_HUMAN
          ******************************************:*********:**:****

P80147    NVSTFINRPALGILPPENFVEKLRESLLSVAPKGMSQLITMACGSCSNENAFKTIFMWYR    180   GABT_PIG
P80404    NASMFVNRPALGILPPENFVEKLRQSLLSVAPKGMSQLITMACGSCSNENALKTIFMWYR    180   GABT_HUMAN
          *.*  *:.***************:.**************************:********

P80147    SKERGQSAFSKEELETCMINQAPGCPDYSILSFMGAFHGRTMGCLATTHSKAIHKIDIPS    240   GABT_PIG
P80404    SKERGQRGFSQEELETCMINQAPGCPDYSILSFMGAFHGRTMGCLATTHSKAIHKIDIPS    240   GABT_HUMAN
          ******  .**:************************************************

P80147    FDWPIAPFPRLKYPLEEFVKENQQEEARCLEEVEDLIVKYRKKKKTVAGIIVEPIQSEGG    300   GABT_PIG
P80404    FDWPIAPFPRLKYPLEEFVKENQQEEARCLEEVEDLIVKYRKKKKTVAGIIVEPIQSEGG    300   GABT_HUMAN
          ************************************************************

P80147    DNHASDDFFRKLRDISRKHGCAFLVDEVQTGGGSTGKFWAHEHWGLDDPADVMTFSKKMM    360   GABT_PIG
P80404    DNHASDDFFRKLRDIARKHGCAFLVDEVQTGGGCTGKFWAHEHWGLDDPADVMTFSKKMM    360   GABT_HUMAN
          ***************:****************.*************************

P80147    TGGFFHKEEFRPNAPYRIFNTWLGDPSKNLLLAEVINIIKREDLLSNAAHAGKVLLTGLL    420   GABT_PIG
P80404    TGGFFHKEEFRPNAPYRIFNTWLGDPSKNLLLAEVINIIKREDLLNNAAHAGKALLTGLL    420   GABT_HUMAN
          *********************************************.*******.******

P80147    DLQARYPQFISRVRGRGTFCSFDTPDESIRNKLISIARNKGVMLGGCGDKSIRFRPTLVF    480   GABT_PIG
P80404    DLQARYPQFISRVRGRGTFCSFDTPDDSIRNKLILIARNKGVVLGGCGDKSIRFRPTLVF    480   GABT_HUMAN
          **************************:.*******  *******:.**************

P80147    RDHHAHLFLNIFSDILADFK    500    GABT_PIG
P80404    RDHHAHLFLNIFSDILADFK    500    GABT_HUMAN
          ********************
```

Figure 4. Comparison of the results of the three different secondary structure prediction servers (JPRED, PSIPRED and SABLE).

Figure 5. Ribbon representation of the modeled GABA-AT protein using Rasmol visualization software.

Figure 6. Sequence model coverage.
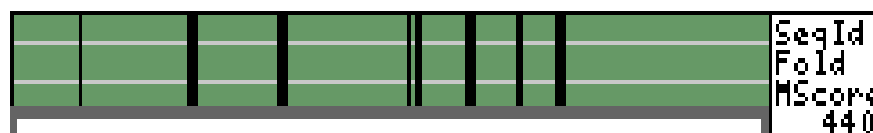
Figure 7. Sequence model coverage (including ligand binding residues).

Putative ligand binding sites derived from 1ohvA

Ligand: ACT
(acetate ion)
Residues

MODEL I39 F156 R159 E237 K296
TEMPL I72 F189 R192 E270 K329

Ligand: PLP
(pyridoxal-5'-phosphate)
Residues

MODEL C102 G103 S104 N107 F156 H157 G158 E232 S236 E237 D265 V267 Q268 S295 K296
TEMPL C135 G136 S137 N140 F189 H190 G191 E265 S269 E270 D298 V300 Q301 S328 K329

Ligand: ACT
(acetate ion)
Residues

MODEL F318 N319 T320
TEMPL F351 N352 T353

Ligand: PLP
(pyridoxal-5'-phosphate)
Residues

MODEL N319 T320 W321
TEMPL N352 T353 W354

Figure 8. Putative ligand binding sites derived from 1ohvA.

third line and is green if model score ≥0.7 and is red if < 0.7 (Pieper et al., 2004). The modeled region is represented by the last line of the sketch (Pieper et al., 2004). In our results, the model coverage sketch showed the 3 lines in green which made it a more reliable predicted structure. The sketch is shown in Figure 6.

The putative ligand binding sites of MODBASE models were derived from the template. Figure 7 displays the same information as the general model coverage sketch. Additionally, it displays the position of the amino acid residues which are putative ligand binding residues as shown in Figure 8. The 3D coordinate file of the model in PDB format was generated after comparative modeling of the target with the template by MODWEB shown in Figure 9. This PDB file was viewed using visual molecular dynamics (VMD) software and Rasmol. The overall summary of GABA-AT protein obtained from SWISSMODEL and MODWEB was classified as 22 strands, 21 helices and 44 turns and number of hydrogen bonds was 317. The results from SWISS MODEL and the predicted protein almost coincided to be exactly and also showed a high degree of conservity to the template used. ANOLEA, GROMOS and VERIFY 3D were used to validate the model (Figure 10).

Sequence Identity	96.00%
E-Value	0
Model Score	1.00
Target Region	1-439
Protein Length	440
Template PDB Code	1ohvA
Template Region	33-471
MPQS	2.14803
z-Dope	-0.98
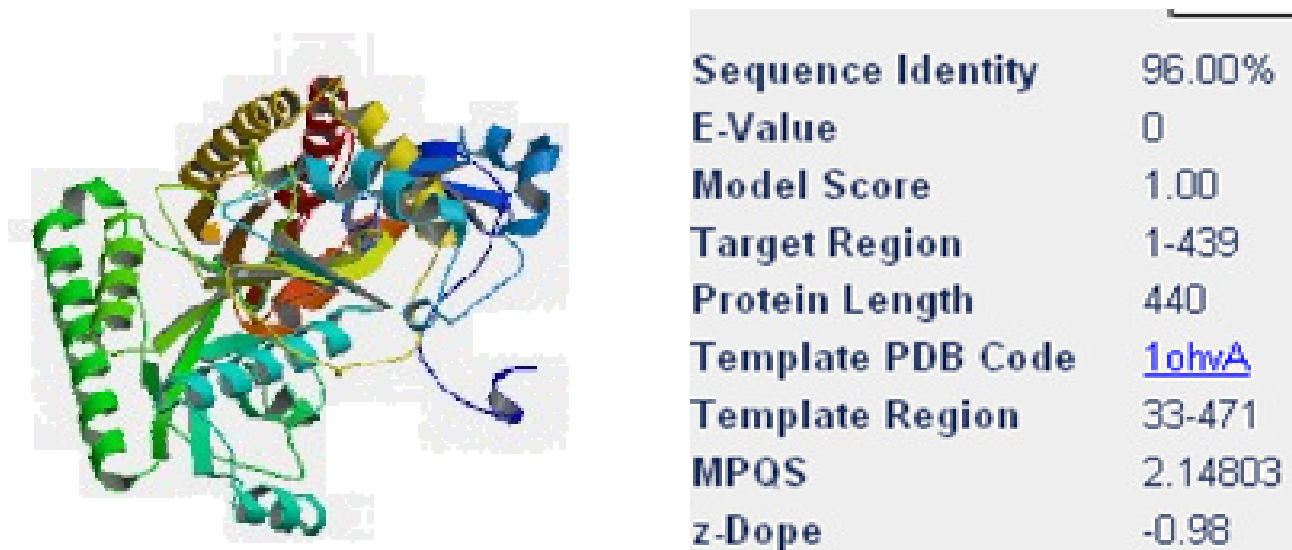
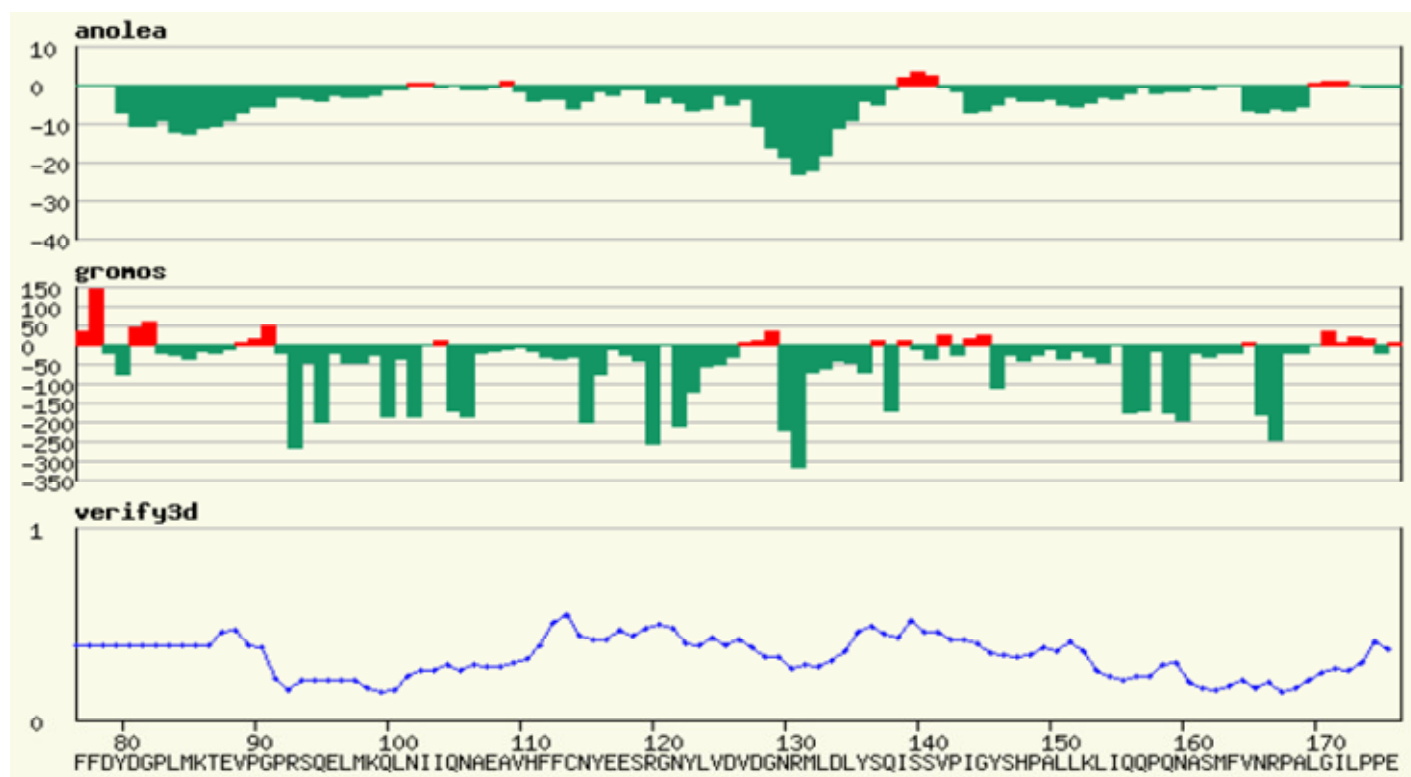**Figure 9.** Ribbon representation of the modeled GABA-AT protein using ModWeb along the protein's important information.

Figure 10. Cont'd.

Future perspective

Knowledge of the three-dimensional structure of GABA-AT would greatly advance the development of novel lead compounds targeting this molecule. As the structure of GABA-AT protein is known from this study, novel lead compounds can be designed on the basis of ligand protein interaction (docking) scores of available anti-epileptic drugs defining the highest dockable compound and designing various analogues of the presently available drugs or defining a novel molecule on the basis of different binding sites. This will be useful for further
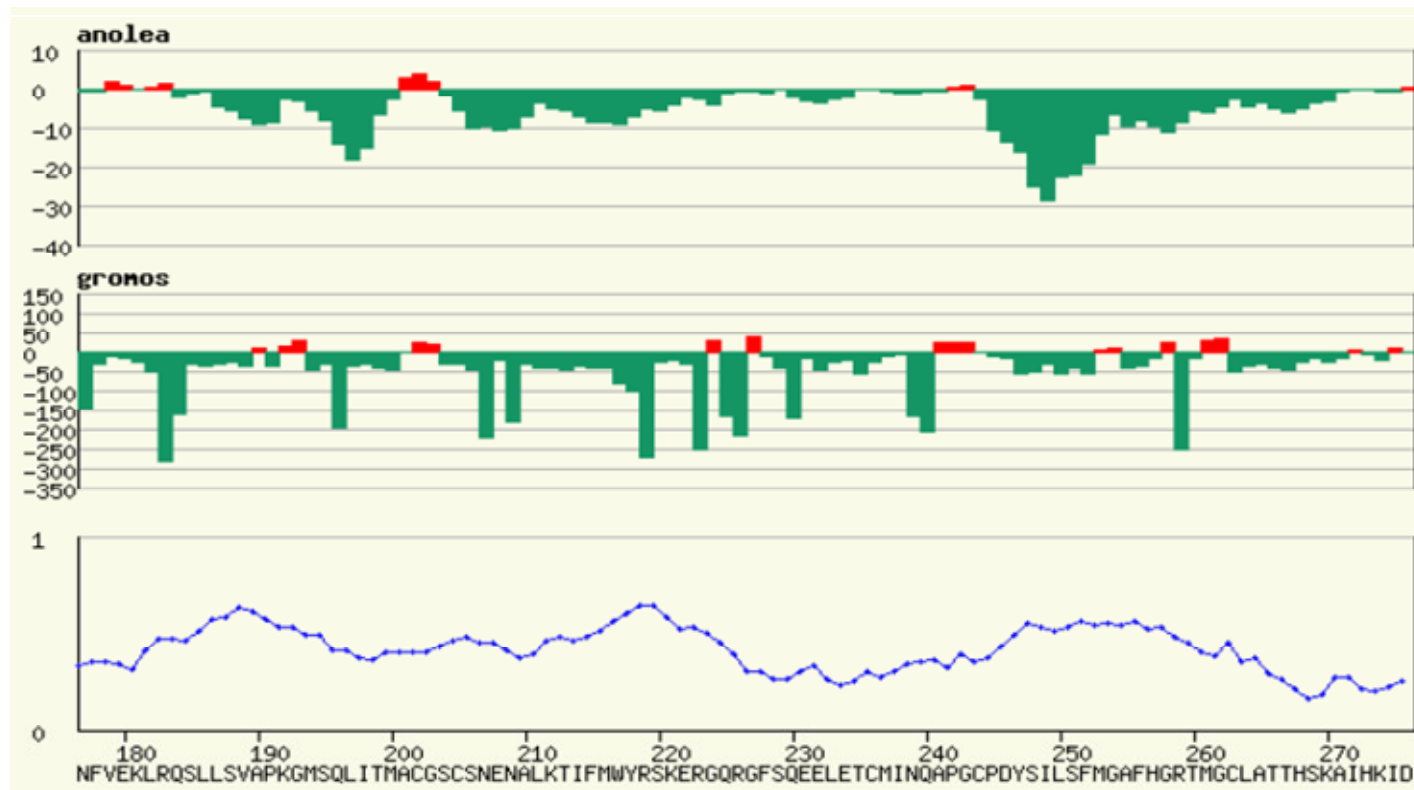
Figure 10. Verification of 3D structure using Anolea, Gromos and Verify3D.

protein-protein interaction prediction, protein-protein docking, molecular docking and pharmacological studies. However, before using the model for further work, it should be checked for its geometrical, stereo chemical and conformational accuracy before taking up for rational drug design, to avoid later complications.

REFERENCES

Adamczak R, Porollo A, Meller J (2005). Combining Prediction of Secondary Structure and Solvent Accessibility in Proteins. Proteins: Structure, Function Bioinformatics, 59: 467-75.

Aoyagi T, Wada T, Nagai M, Kojima F, Harada S, Takeuchi T, Takahashi H, Hirokawa K, Tsumita, T (1990). Increased γ-aminobutyrate aminotransferase activity in brain patients with Alzheimer's disease. Chem. Pharm. Bull., 38: 1748–1749.

Bairoch A, Bucher P, Hofmann K (1997). PROSITE: Nucleic Acids Res., 25: 217-221.

Bajorath J, Stenkamp R, Aruffo A (1994). Knowledge-based model building of proteins: Concepts and examples. Protein Sci., 2: 1798–1810.

Bakay RAE, Harris AB (1981). Neurotransmitter, receptor and biochemical changes in monkey cortical epileptic foci. Brain Res., 206: 387-404.

Bell GS, Sander JW (2001). The epidemiology of epilepsy: the size of the problem. Seizure, 10: 306–316.

Bloch-Tardy M, Rolland B, Gonnard P (1974). Kinetic and thermodynamic studies with NADH as coenzyme. Biochimie, 56: 823-832.

Blundell TL, Sibanda BL, Sternberg MJE, Thornton JM (1987). Knowledge-based prediction of protein structures and the design of novel molecules. Nature, 326: 347–352.

Butterworth J, Yates CM, Simpson J (1983). Phosphate-activated glutaminase in relation to Huntington's disease and agonal state. J Neurochem., 41: 440–447

Ceroni A, Frasconi P, Passerini A, Vullo A (2004). Disulfide connectivity prediction using recursive neural networks and evolutionary information. Bioinformatics, 20: 653-659.

Cole C, Barber JD, Barton GJ (2008). The Jpred 3 secondary structure prediction server. Nucleic Acids Res., 36: 197–201.

Cooper AJ (1985). Glutamate-gamma-aminobutyrate transaminase. Methods Enzymol., 113: 80-82.

Davies JA (1995). Mechanisms of action of antiepileptic drugs. Seizure, 4: 267-271.

De Biase D, Barra D, Simmaco M, John RA, Bossa F (1995). Primary structure and tissue distribution of human 4-aminobutyrate aminotransferase. Eur. J. Biochem., 227: 476-480.

Edgar RC (2004). MUSCLE: multiple sequence alignment with high accuracy and high throughput. Nucleic Acids Res., 32(5): 1792-1797.

Enyedy I, Lee S, Kuo A., Dickson R, Lin C, Wang S (2001). Structure-based approach for the discovery of bisbenzamidines as novel inhibitors of matriptase. J. Med. Chem., 44: 1349–1355.

Greer J (1990). Comparative modelling methods: Application to the family of the mammalian serine proteases. Proteins, 7: 317–334.

Gunne LM, Haeggstroem JE, Sjoequist B (1984). Association with persistent neurolepticinduced dyskinesia of regional. Nature, 309: 347–349.

Hirokawa T, Boon CS, Mitaku S (1998). SOSUI: classification and secondary structure prediction system for membrane proteins. Bioinformatics, 14: 378-379.

Hofmann K, Stoffel W (1993). TMbase - A database of membrane spanning proteins segments. Biol Chem 374: 166-170.

Holm L, Sander C (1992). Evaluation of protein models by atomic salvation preference; J. Mol. Biol., 225: 93-105.

Jain AN (2004). Virtual screening in lead discovery and optimization. Curr. Opin. Drug Discov. Dev., 7: 396–403.

Johnson MS, Srinivasan N, Sowdhamini R, Blundell TL (1994).

Knowledge-based protein modelling. CRC Crit. Rev. Biochem. Mol. Biol., 29: 1–68.

Kasteleijn-Nolst Trenité DGA, Genton P, Parain D, Masnou P, Steinhoff BJ, Jacobs T (2007). Evaluation of brivaracetam, a novel SV2A ligand, in the photosensitivity model. Neurology, 69: 1027-1034.

Krogh A, Larsson B, Von HG, EL Sonnhammer (2001). Predicting transmembrane protein topology with a hidden Markov model: application to complete genomes. J. Mol. Biol., 305: 567-80.

Laskowski RA, MacArthur MW, Moss DS, Thornton JM (1993). PROCHECK: a program to check the stereochemical quality of protein structures; J. Appl. Cryst., 26: 283-291.

Lippert B, Metcalf BW, Jung M.J, Casara P (1977). 4-amino-hex-5-enoic acid: a selective catalytic inhibitor of 4-aminobutyric acid aminotransferase in mammalian brain. Eur. J. Biochem. ,74: 441-445.

McGuffin LJ, Bryson K and Jones DT (2000). The PSIPRED protein structure prediction server. Bioinformatics Appl. Note, 16: 404-405.

Mehta PK, Christen P (2000). The molecular evolution of pyridoxal-5'-phosphate-dependent enzymes. Adv. Enzymol. Relat. Areas Mol. Biol., 74: 129–184.

Mehta PK, Hale TI, Christen P (1993). Aminotransferases: demonstration of homology and division into evolutionary subgroups. Eur. J. Biochem., 214: 549-561.

Nishino N, Fujiwara H, Noguchi-Kuno SA, Tanaka C (1988). GABA$_A$ receptor but not muscarinic receptor density was decreased in the brain of patients with Parkinson's disease. Jpn. J. Pharmacol., 48: 331-339.

Pieper U, Eswar N, Braberg H, Madhusudhan MS, Davis FP, Stuart AC, Mirkovic N, Ossi A, Marti-Renom M, Fiser A, Webb B, Greenblatt D, Huang CC, Ferrin TE, Sali A (2004). MODBASE, a database of annotated comparative protein structure models, and associated resources. Nucleic Acids Res., 32: 217-222.

Pieper U, Eswar N, Webb BM, Eramian D, Kelly L, Barkan DT, Carter H, Mankoo P, Karchin R, Marti-Renom MA, Davis FP and Sali A (2009). MODBASE, a database of annotated comparative protein structure models and associated resources. Nucleic Acids Res., 37:347-354.

Puntervoll P, Linding R, Gemünd C, Chabanis DS, Mattingsdal M, et al. (2003). ELM server: a new resource for investigating short functional sites in modular eukaryotic proteins. Nucleic Acids Res., 31: 3625-3630.

Rogawski MA, Porter RJ (1990). Antiepileptic drugs: pharmacological mechanisms and clinical efficacy with consideration of promising developmental stage compounds. Pharmacol. Rev., 42: 223–286.

Rost B, Yachdav G, Liu J (2004). The PredictProtein Server. Nucleic Acids Res., 32: 321-326.

Sali A (1995). Modelling mutations and homologous proteins. Curr. Opin. Biotech., 6: 437–451.

Sali A, Blundell TL (1993). Comparative protein modelling by satisfaction of spatial restrainsts; J. Mol. Biol., 234: 779-815.

Sanchez R, Sali A (1997). Advances in comparative protein-structure modeling. Curr. Opin. Struct. Biol., 7: 206–214.

Shankar R, Frapaise X, Brown B (2006). LEAN drug development in R&D. Drug Discov Dev., pp. 57–60.

Stoermer MJ (2006). Current status of virtual screening as analysed by target class. Med. Chem., 2: 89–112.

Storici P, Qiu J, Schirmer T, Silverman RB (2004). Mechanistic crystallography. Mechanism of inactivation of gamma-aminobutyric acid aminotransferase by (1R,3S,4S)-3-amino-4-fluorocyclopentane-1-carboxylic acid as elucidated by crystallography. Biochemistry, 43(44): 14057–14063.

Thompson JD, Higgins DG, Gibson TJ (1994). CLUSTAL W: improving the sensitivity of progressive multiple sequence alignment through sequence weighting, position-specific gap penalties and weight matrix choice. Nucleic Acids Res., 22: 4673-4680.